

## ARTICLES

## Efficient Catalysis of Rare-Earth Metal Ions in Photoinduced Electron-Transfer Oxidation of Benzyl Alcohols by a Flavin Analogue

Shunichi Fukuzumi,<sup>\*,†</sup> Kiyomi Yasui,<sup>†</sup> Tomoyoshi Suenobu,<sup>†</sup> Kei Ohkubo,<sup>†</sup> Mamoru Fujitsuka,<sup>‡</sup> and Osamu Ito<sup>‡</sup>

Department of Material and Life Science, Graduate School of Engineering, Osaka University, CREST, Japan Science and Technology Corporation (JST), Suita, Osaka 565-0871, Japan, and Institute of Multidisciplinary Research for Advanced Materials, Tohoku University, CREST, Japan Science and Technology Corporation (JST), Sendai, Miyagi 980-8577, Japan

Received: July 13, 2001

A flavin analogue (riboflavin-2',3',4',5'-tetraacetate, Fl) forms the 1:1 and 1:2 complexes with rare-earth metal ions. The largest formation constants  $K_1$  and  $K_2$  for the 1:1 and 1:2 complexes between Fl and  $\text{Sc}^{3+}$  are determined as  $K_1 = 3.1 \times 10^4 \text{ M}^{-1}$  and  $K_2 = 1.4 \times 10^3 \text{ M}^{-1}$ , respectively. The complexation of Fl with rare-earth metal ions results in blue shifts of the fluorescence maximum, shortening of the fluorescence lifetime, and more importantly the change in the lowest excited state from the  $n, \pi^*$  triplet state of Fl to the  $\pi, \pi^*$  singlet states of Fl–rare-earth metal ion complexes as indicated by the disappearance of the triplet–triplet (T–T) absorption spectrum of Fl by the complexation with metal ions. The strong complex formation between Fl and rare-earth metal ions enhances the oxidizing ability of the excited state of Fl as indicated by the significant acceleration in the fluorescence quenching rates of Fl–rare earth metal ion complexes via electron transfer from electron donors (e.g., alkylbenzenes) as compared to those of uncomplexed Fl. The one-electron reduction potential of the singlet excited state of the 1:2 complex between Fl and  $\text{Sc}^{3+}$ ,  $^1(\text{Fl}-2\text{Sc}^{3+})^*$  (\* denotes the excited state), is positively shifted by 780 mV as compared to  $^1\text{Fl}^*$ . Such a remarkable enhancement of the redox reactivity of  $^1(\text{Fl}-2\text{Sc}^{3+})^*$  as compared to that of  $^1\text{Fl}^*$  makes it possible to oxidize efficiently *p*-chlorobenzyl alcohol to *p*-chlorobenzaldehyde by  $^1(\text{Fl}-2\text{Sc}^{3+})^*$ , although no photooxidation of *p*-chlorobenzyl alcohol by Fl occurred in deaerated MeCN. The quantum yield for the photooxidation of *p*-chlorobenzyl alcohol by Fl– $2\text{Sc}^{3+}$  is the largest among various Fl–metal ion complexes. A comparison of the observed rate constant derived from the dependence of the quantum yield on the concentration of *p*-chlorobenzyl alcohol with the fluorescence quenching rate constant by electron transfer from the alcohol and the direct detection of radical intermediates reveal that the photooxidation proceeds via electron transfer from *p*-chlorobenzyl alcohol to  $^1(\text{Fl}-2\text{Sc}^{3+})^*$ . Under an atmospheric pressure of oxygen, the photooxidation of *p*-methoxybenzyl alcohol by oxygen proceeds efficiently in the presence of Fl– $\text{Lu}^{3+}$  which acts as an efficient photocatalyst. No photodegradation was observed in the case of the Fl– $\text{Lu}^{3+}$  complex, whereas the facile photodegradation of Fl– $\text{Mg}^{2+}$  has precluded the efficient photocatalytic oxidation of the alcohol by oxygen.

## Introduction

Flavoenzymes are a ubiquitous and structurally and functionally diverse class of redox-active proteins that use the redox active isoalloxazine ring of flavins to mediate a variety of electron-transfer processes over a wide range of redox potentials.<sup>1</sup> The redox reactivity of flavins is modulated by the interaction with apoenzymes, that is affected by hydrogen-bonding,<sup>1,2</sup>  $\pi$ – $\pi$  stacking,<sup>3</sup> donor– $\pi$  interaction,<sup>4</sup> conformational effects,<sup>5</sup> and coordination to metal ions.<sup>6</sup> Although direct

determination of the roles of these noncovalent interactions in biological systems has been complicated by the multiple forces involved, model studies have provided valuable information to probe and isolate each of these interactions.<sup>7</sup> The redox reactivity of flavins is the most drastically changed by the photoexcitation as compared to the ground state. Thus, photochemistry of flavoenzymes and flavin analogues has been the subject of intense research in photocatalysts for the photobiological redox processes.<sup>8–10</sup> The redox reactivity of the photoexcited states of flavins has been further modulated by coordination to metal ions.<sup>11–13</sup> Divalent metal cations ( $\text{Mg}^{2+}$ ,  $\text{Ca}^{2+}$ ,  $\text{Sr}^{2+}$ ,  $\text{Ba}^{2+}$ ,  $\text{Zn}^{2+}$ , or  $\text{Cd}^{2+}$ ) have been reported to be indispensable for the flavin-dependent photocleavage of RNA at particular base pairs via oxidative cleavage processes.<sup>14</sup> The effect of metal ions on the photocatalytic reactivity has also been studied using flavin

\* Author to whom correspondence should be addressed. E-mail: fukuzumi@ap.chem.eng.osaka-u.ac.jp.

<sup>†</sup> Osaka University, CREST, Japan Science and Technology Corporation (JST).

<sup>‡</sup> Tohoku University, CREST, Japan Science and Technology Corporation (JST).

analogues with the crown ether moiety as binding site for metal ions.<sup>15</sup>

Among metal ions, rare-earth metal ions have attracted considerable interest as mild and selective Lewis acids in organic synthesis.<sup>16</sup> Trivalent rare-earth ( $\text{Sc}^{3+}$ ,  $\text{Yb}^{3+}$ , etc.) trifluoromethanesulfonates (triflates) have been utilized as Lewis acids in promoting various carbon–carbon bond forming reactions.<sup>17</sup> In particular, scandium(III) triflate [ $\text{Sc}(\text{OTf})_3$ ] has attracted much attention due to its hard character as well as strong affinity to carbonyl oxygen.<sup>18</sup> However, there has been no report on the effects of rare-earth metal ions on the redox reactivity of photoexcited states of flavins and the photocatalytic reactivity.

We report herein that the riboflavin-2',3',4',5'-tetraacetate (Fl) forms not only 1:1 but also 1:2 complexes with rare-earth metal ions and that the Fl–rare-earth metal ion complexes can act as efficient photocatalysts possessing much stronger oxidizing ability as well as much improved stability against the photo-degradation as compared to the Fl–divalent metal ion ( $\text{Mg}^{2+}$ ) complex in the photocatalytic oxidation of benzyl alcohol derivatives by oxygen. Remarkable enhancement in the redox reactivity of the photoexcited state of Fl–rare-earth metal ion complexes has been evaluated quantitatively as compared to the Fl– $\text{Mg}^{2+}$  complex and the uncomplexed Fl by analyzing the free energy relationships for the photoinduced electron-transfer reactions. Since we have found that the 1:2 complex formed between Fl and  $\text{Sc}^{3+}$  (Fl– $2\text{Sc}^{3+}$ ) shows the largest reactivity among the Fl–metal ion complexes, the reaction mechanisms for the photooxidation of benzyl alcohol derivatives by Fl– $2\text{Sc}^{3+}$  and the photocatalytic oxidation by oxygen are revealed based on the dependence of quantum yields on the alcohol concentration and the direct detection of the reactive intermediates in the photochemical reaction by the laser flash photolysis of the Fl– $2\text{Sc}^{3+}$ /benzyl alcohol derivative system.

## Experimental Section

**Materials.** Flavin analogue (riboflavin-2',3',4',5'-tetraacetate, Fl) was prepared by the reaction of riboflavin obtained from Wako Pure Chemicals with acetic anhydride in pyridine and purified by recrystallization from ethanol–chloroform.<sup>19</sup> Benzene derivatives (toluene, ethylbenzene, *m*-xylene, *o*-xylene, *p*-cymene, *p*-xylene, 1,2,3-trimethylbenzene, 1,2,4-trimethylbenzene, 1,2,3,5-tetramethylbenzene, 1,2,3,4-tetramethylbenzene, pentamethylbenzene, and *m*-dimethoxybenzene) used as electron donors in fluorescence quenching experiments were obtained from Tokyo Kasei Organic Chemicals. *p*-Methoxybenzyl alcohol, *p*-chlorobenzyl alcohol, *p*-methoxybenzaldehyde, and *p*-chlorobenzaldehyde were obtained from Tokyo Kasei Organic Chemicals. Potassium ferrioxalate used as an actinometer was prepared according to the literature,<sup>20</sup> and purified by recrystallization from hot water. Anhydrous magnesium perchlorate was obtained from Nacalai Tesque. Scandium triflate [ $\text{Sc}(\text{OTf})_3$ ] was prepared by the following procedure according to the literature.<sup>21</sup> A deionized aqueous solution was mixed (1:1 v/v) with trifluoromethanesulfonic acid (>99.5%, 10.6 mL) obtained from Central Glass, Co., Ltd., Japan. The trifluoromethanesulfonic acid solution was slowly added to a flask which contained scandium oxide ( $\text{Sc}_2\text{O}_3$ ) (>99.9%, 30 mmol) obtained from Shin-Etsu Chemical, Co., Ltd., Japan. The mixture was refluxed at 100 °C for 3 days. After centrifugation of the reaction mixture, the solution containing scandium triflate was separated and water was removed by vacuum evaporation. Scandium triflate was dried under vacuum evacuation for 40 h. Similarly, lutetium triflate and ytterbium triflate were prepared by the reaction of lutetium oxide and ytterbium oxide with an aqueous

solution of trifluoromethanesulfonic acid. Lanthanum triflate was obtained from Aldrich as hexahydrate form and used after drying under vacuum evacuation for 40 h. Magnesium triflate [ $\text{Mg}(\text{OTf})_2$ ] obtained from Aldrich was used as received. 1-Benzyl-1,4-dihydropyridinamide dimer [(BNA)<sub>2</sub>] was prepared according to the literature.<sup>22</sup> Acetonitrile used as a solvent was purified and dried by the standard procedure.<sup>23</sup> Acetonitrile-*d*<sub>3</sub> and chloroform-*d* were obtained from EURISO-TOP, CEA, France.

**Reaction Procedures and Analysis.** Typically, Fl ( $1.0 \times 10^{-2}$  M) was added to an NMR tube that contained an acetonitrile-*d*<sub>3</sub> ( $\text{CD}_3\text{CN}$ ) solution (0.6 mL) of *p*- $\text{ClC}_6\text{H}_4\text{CH}_2\text{OH}$  ( $2.0 \times 10^{-2}$  M) in the presence of  $\text{Sc}(\text{OTf})_3$  ( $3.0 \times 10^{-2}$  M). Then the solution was deaerated by bubbling with argon gas for 5 min, and the NMR tube was sealed with a rubber septum. The solution was irradiated with a xenon lamp (USHIO-UI-501C) through Pyrex filter transmitting  $\lambda > 420$  nm for 9 h. The oxidation product of *p*- $\text{ClC}_6\text{H}_4\text{CH}_2\text{OH}$  was identified by comparing the <sup>1</sup>H NMR spectrum with that of an authentic sample of *p*- $\text{ClC}_6\text{H}_4\text{CHO}$ . The yield of the reaction was determined on the basis of the concentration of the internal standard, 1,4-dioxane ( $2.0 \times 10^{-3}$  M). <sup>1</sup>H NMR measurements were performed with a Japan Electron Optics JNM-GSX-400 (400 MHz) NMR spectrometer at 300 K. <sup>1</sup>H NMR ( $\text{CD}_3\text{CN}$ , 298 K);  $\delta(\text{Me}_4\text{Si}, \text{ppm})$ : *p*- $\text{ClC}_6\text{H}_4\text{CHO}$ ,  $\delta$  7.5 (m, 2H), 7.8 (m, 2H), 9.9 (s, 1H, CHO). The photooxidation of *p*- $\text{MeOC}_6\text{H}_4\text{CH}_2\text{OH}$  with Fl in the presence of  $\text{Lu}(\text{OTf})_3$  in oxygen-saturated MeCN was performed as follows. Typically, *p*- $\text{MeOC}_6\text{H}_4\text{CH}_2\text{OH}$  ( $3.0 \times 10^{-3}$  M) was added to the MeCN solution of Fl ( $2.0 \times 10^{-4}$  M) in the presence of  $\text{Lu}(\text{OTf})_3$  ( $1.0 \times 10^{-2}$  M) in quartz cuvette (i.d. 10 mm). The solution was purged with oxygen gas for 5 min and irradiated with the monochromatized light ( $\lambda = 430$  nm, Slit width: 20 nm) from a SHIMADZU spectrofluorophotometer (RF-5000). The aliquot of reaction solution was diluted and introduced to a SHIMADZU gas chromatography–mass spectrometer system (GC 17A–QP 5000) to measure the amount of the oxidation product, *p*- $\text{MeOC}_6\text{H}_4\text{CHO}$  and the reactant, *p*- $\text{MeOC}_6\text{H}_4\text{CH}_2\text{OH}$ . The amount of reduction product  $\text{H}_2\text{O}_2$  was determined by the standard method (titration by iodide ion);<sup>24</sup> the diluted MeCN solution of the product mixture was treated with excess amounts of NaI and the amount of  $\text{I}_3^-$  formed was determined by the visible spectrum ( $\lambda_{\text{max}} = 362$  nm,  $\epsilon = 1.3 \times 10^4 \text{ M}^{-1} \text{ cm}^{-1}$ ) with use of a Hewlett-Packard 8452A diode array spectrophotometer.

**Spectral Measurements.** The formation of Fl–rare-earth ion complexes was examined from the change in the UV–Vis spectra of Fl ( $1.0 \times 10^{-4}$  M) in the presence of various concentrations of  $\text{Yb}(\text{OTf})_3$  ( $6.6 \times 10^{-5}$ – $2.7 \times 10^{-3}$  M),  $\text{Lu}(\text{OTf})_3$  ( $6.6 \times 10^{-5}$ – $2.7 \times 10^{-3}$  M),  $\text{La}(\text{OTf})_3$  ( $6.6 \times 10^{-5}$ – $2.8 \times 10^{-3}$  M),  $\text{Mg}(\text{OTf})_2$  ( $1.0 \times 10^{-4}$ – $5.0 \times 10^{-1}$  M), and  $\text{Sc}(\text{OTf})_3$  ( $6.5 \times 10^{-6}$ – $7.3 \times 10^{-4}$  M) with use of a Hewlett-Packard 8452A diode array spectrophotometer. The formation constants were obtained from the change in the UV–Vis spectra due to the formation of the 1:1 complexes: Fl– $\text{Yb}^{3+}$  ( $\lambda_{\text{max}} = 376$  and 430 nm), Fl– $\text{Lu}^{3+}$  ( $\lambda_{\text{max}} = 362$  and 438 nm), Fl– $\text{La}^{3+}$  ( $\lambda_{\text{max}} = 370$  and 434 nm), Fl– $\text{Mg}^{2+}$  ( $\lambda_{\text{max}} = 360$  and 436 nm), and the 1:2 complex, Fl– $2\text{Sc}^{3+}$  ( $\lambda_{\text{max}} = 384$  and  $\lambda_{\text{max}} = 426$  nm). The measurements of IR spectra of rare-earth ion complexes with Fl (Fl– $2\text{Sc}^{3+}$ , Fl– $\text{Yb}^{3+}$ , and Fl– $\text{Mg}^{2+}$ ) in MeCN were performed on a SHIMADZU-FTIR8200PC spectrophotometer. A standard actinometer (potassium ferrioxalate)<sup>20</sup> was used for the quantum yield determinations on the photochemical reaction of Fl with *p*- $\text{ClC}_6\text{H}_4\text{CH}_2\text{OH}$  under a deaerated condition in the presence of  $\text{Sc}^{3+}$  ion as well as the photooxi-

dation of *p*-MeOC<sub>6</sub>H<sub>4</sub>CH<sub>2</sub>OH by oxygen catalyzed by FI in the presence of Lu<sup>3+</sup> ion in MeCN. In the case of photooxidation of *p*-ClC<sub>6</sub>H<sub>4</sub>CH<sub>2</sub>OH with FI, a square quartz cuvette (10 mm i.d.) which contained a deaerated MeCN solution of FI (1.0 × 10<sup>-2</sup> M) and *p*-ClC<sub>6</sub>H<sub>4</sub>CH<sub>2</sub>OH (1.0 × 10<sup>-2</sup> – 8.0 × 10<sup>-1</sup> M) in the presence of Sc(OTf)<sub>3</sub> (1.0 × 10<sup>-2</sup> M) was irradiated with the monochromatized light (λ = 430 nm) with the slit width of 20 nm from a SHIMADZU spectrofluorophotometer (RF-5000) at 298 K. The light intensity of monochromatized light of λ = 430 nm was determined as 4.7 × 10<sup>-8</sup> einstein s<sup>-1</sup> with the slit width of 20 nm. The photochemical reaction was monitored by a Hewlett-Packard 8452A diode array spectrophotometer. The quantum yields in deaerated condition were determined from the decrease in absorbance due to FI at λ<sub>max</sub> = 430 nm in MeCN. The quantum yields for the photooxidation of *p*-MeOC<sub>6</sub>H<sub>4</sub>CH<sub>2</sub>OH by oxygen in the presence of Lu<sup>3+</sup> ion in MeCN were determined from the increase in absorption band at λ = 350 nm due to the product *p*-MeOC<sub>6</sub>H<sub>4</sub>CHO which is identified by the GC-MS analysis.

**Fluorescence Quenching Experiments.** Quenching experiments of the fluorescence of FI–metal ion complexes were carried out on a SHIMADZU spectrofluorophotometer (RF-5000). The excitation wavelength of FI and FI–metal ion complexes (FI–2Sc<sup>3+</sup>, FI–Yb<sup>3+</sup>, and FI–Mg<sup>2+</sup>) was 460 nm in deaerated and aerated MeCN. The monitoring wavelengths were those corresponding to the maxima of the emission band at λ<sub>max</sub> = 486 nm (FI–2Sc<sup>3+</sup>), λ<sub>max</sub> = 500 nm (FI–Yb<sup>3+</sup>), λ<sub>max</sub> = 504 nm (FI–Mg<sup>2+</sup>), and λ<sub>max</sub> = 506 nm (FI). The MeCN solutions were deaerated by argon purging for 7 min prior to the measurements. Relative fluorescence intensities were measured for MeCN solutions containing FI (1.0 × 10<sup>-5</sup> M) with various alkylbenzenes (1.0 × 10<sup>-2</sup> – 9.6 × 10<sup>-1</sup> M) in the absence and presence of metal ions (1.0 × 10<sup>-2</sup> M). There was no change in the shape but there was a change in the intensity of the fluorescence spectrum by the addition of a quencher. The Stern–Volmer relationship (eq 1)

$$I_0/I = 1 + K_q[D] \quad (1)$$

was obtained for the ratio of the fluorescence intensities (*I*<sub>0</sub>/*I*) in the absence and presence of electron donors and the concentrations of donors used as quenchers [D]. The fluorescence lifetimes (τ) of the metal ion complexes of FI were determined in deaerated MeCN containing metal ions at 298 K by single photon counting using a Horiba NAES-1100 time-resolved spectrofluorophotometer.

**Laser Flash Photolysis.** Triplet–triplet transient absorption spectra of FI and FI–Yb<sup>3+</sup> complex were measured by laser flash photolysis of the MeCN solution containing FI (1.0 × 10<sup>-5</sup> M) in the absence and presence of Yb(OTf)<sub>3</sub> (1.0 × 10<sup>-2</sup> M). For the detection of transient absorption spectra in the photochemical reaction of the FI–Sc(OTf)<sub>3</sub> complex with *p*-ClC<sub>6</sub>H<sub>4</sub>CH<sub>2</sub>OH, a deaerated MeCN solution containing FI (1.0 × 10<sup>-4</sup> M), *p*-ClC<sub>6</sub>H<sub>4</sub>CH<sub>2</sub>OH (1.0 M), and Sc(OTf)<sub>3</sub> (1.0 × 10<sup>-2</sup> M) was excited by an optical parametric oscillation (Continuum Surelite OPO, fwhm 4 ns, 440 nm) pumped by a Nd:YAG laser (Continuum, Surelite II-10) with the power of 10 mJ. For the photoinduced electron transfer from (BNA)<sub>2</sub> to the FI–Sc(OTf)<sub>3</sub> complex, (BNA)<sub>2</sub> (1.0 × 10<sup>-4</sup> M) was employed in place of *p*-ClC<sub>6</sub>H<sub>4</sub>CH<sub>2</sub>OH under otherwise the same experimental conditions. The transient spectra were recorded using fresh solutions in each laser excitation. All experiments were performed at 298 K.

**Electrochemical Measurement.** Redox potentials of various benzene derivatives (2.0 × 10<sup>-3</sup> M) in MeCN containing 0.10

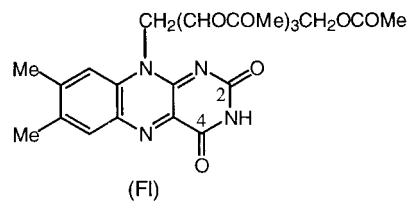
M TBAP as a supporting electrolyte were determined at room temperature by SHACV (second harmonic ac voltammetry) method<sup>25</sup> under deaerated conditions using a three-electrode system and a BAS 100B electrochemical analyzer. The working and counter electrodes were platinum, while Ag/AgNO<sub>3</sub> (0.01 M) was used as a reference electrode. All potentials (vs Ag/Ag<sup>+</sup>) were converted to values vs SCE by adding 0.29 V.<sup>26</sup>

**ESR Measurements.** FI was dissolved in MeCN (3.3 mg; 6.0 × 10<sup>-3</sup> M in 1.0 mL) and purged with argon for 10 min. Sc(OTf)<sub>3</sub> (9.8 mg; 2.0 × 10<sup>-2</sup> M in 1.0 mL) was also dissolved in deaerated MeCN. The FI solution (200 μL) and Sc(OTf)<sub>3</sub> solution (200 μL) were introduced into the ESR cell (0.8 mm i.d.) containing (BNA)<sub>2</sub> (1.0 mg) and mixed by bubbling with Ar gas through a syringe with a long needle. The ESR spectra of FI<sup>•-</sup>–2Sc<sup>3+</sup> were recorded on a JEOL JES-RE1XE spectrometer under irradiation of a high-pressure mercury lamp (USH-1005D) focusing at the sample cell in the ESR cavity at 298 K. The ESR spectra of FI<sup>•-</sup> were also measured in the absence of Sc(OTf)<sub>3</sub> under otherwise the same experimental conditions. The magnitude of modulation was chosen to optimize the resolution and signal-to-noise (S/N) ratio of the observed spectra under nonsaturating microwave power conditions. The *g* values were calibrated using an Mn<sup>2+</sup> marker.

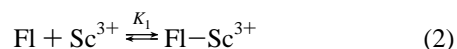
**Theoretical Calculations.** Density functional calculation was performed on a COMPAQ DS20E computer using the spin-restricted B3LYP functional for the open shell molecule.<sup>27</sup> B3LYP geometries for *N*(10)-methyl flavin radical anion were determined using the 6-311++G\*\* basis and the Gaussian 98 program.<sup>28</sup> The ⟨*S*<sup>2</sup>⟩ value was determined as 0.763, indicating a good representation of the doublet state.

## Results and Discussion

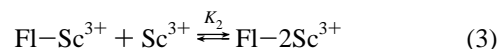
**Complex Formation of FI with Metal Ions.** The UV–Vis absorption spectra of FI in MeCN are significantly affected by the addition of metal ions. The absorption band of FI at 362 nm is red shifted and the absorption band of FI at 438 nm is blue shifted in the presence of metal ions. As shown in Figure 1 for the FI–Sc<sup>3+</sup> complex, isosbestic points are observed at 300, 354, and 425 nm at low concentrations of Sc(OTf)<sub>3</sub>. However, crossover points observed at the low Sc(OTf)<sub>3</sub> concentrations spread over slightly in a progressive manner when the Sc(OTf)<sub>3</sub> concentration was increased and then, new isosbestic points are observed at 302, 362, and 467 nm at higher Sc(OTf)<sub>3</sub> concentration. Such spectroscopic changes may be interpreted as due to the formation of complexes between FI



and Sc(OTf)<sub>3</sub> via two steps. The first step is the formation of a 1:1 complex (eq 2)



and the second step is the additional Sc<sup>3+</sup> coordination to FI for the formation of a 1:2 complex (eq 3).



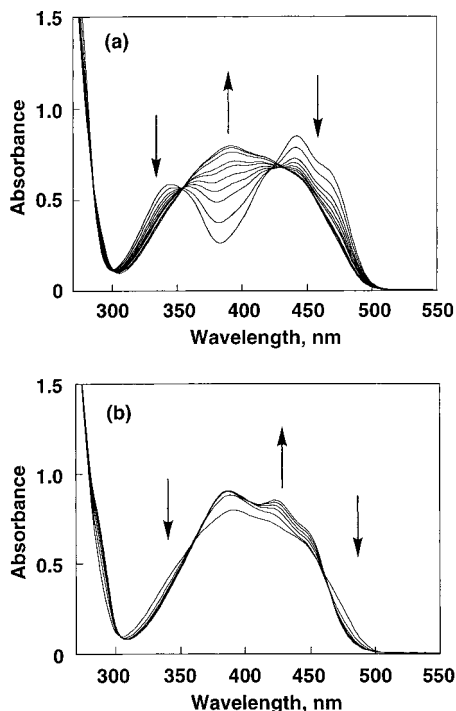


**Figure 1.** Electronic absorption spectra of FI ( $1.0 \times 10^{-4}$  M) in the presence of various concentrations of (a)  $\text{Sc}^{3+}$  ( $0, 1.3 \times 10^{-5}, 2.5 \times 10^{-5}, 3.8 \times 10^{-5}, 5.0 \times 10^{-5}, 6.3 \times 10^{-5}, 7.5 \times 10^{-5}, 1.0 \times 10^{-4}, 1.1 \times 10^{-4}, 1.3 \times 10^{-4}$  M), and (b)  $\text{Sc}^{3+}$  ( $1.3 \times 10^{-4}, 2.5 \times 10^{-4}, 3.7 \times 10^{-4}, 4.9 \times 10^{-4}, 6.1 \times 10^{-4}, 7.3 \times 10^{-4}$  M) in MeCN at 298 K.

Similar two-step spectroscopic changes were also observed when  $\text{Sc}(\text{OTf})_3$  is replaced by  $\text{La}(\text{OTf})_3$  or  $\text{Mg}(\text{ClO}_4)_2$ .

The equilibrium constant ( $K_1$ ) in eq 2 is determined by eq 4,<sup>29</sup>

$$(\alpha^{-1} - 1)^{-1} = K_1([\text{Sc}^{3+}]_0 - \alpha[\text{FI}]_0) \quad (4)$$

where  $[\text{Sc}^{3+}]_0$  and  $[\text{FI}]_0$  are the initial concentrations, and  $\alpha = (A - A_0)/(A_\infty - A_0)$ ;  $A$  is the absorbance at 384 nm in the presence of  $\text{Sc}(\text{OTf})_3$ ,  $A_0$  and  $A_\infty$  are the initial and final absorbances at the same wavelength in the absence and presence of an excess of  $\text{Sc}(\text{OTf})_3$  such that all the FI molecules form the 1:1 complex (FI- $\text{Sc}^{3+}$ ), respectively. The linear plot between  $(\alpha^{-1} - 1)^{-1}$  and  $([\text{Sc}^{3+}]_0 - \alpha[\text{FI}]_0)$  is shown in Figure 2a. The  $K_1$  value is determined from the slope of the linear plot in Figure 2a.

The  $K_2$  value in eq 3 is determined using the  $K_1$  value as follows. The absorbance  $A'$  at 452 nm due to the FI- $2\text{Sc}^{3+}$  complex is expressed by eq 5,

$$\{(1 + K_1[\text{Sc}^{3+}]_0)A' - A_0'\}/K_1[\text{Sc}^{3+}]_0 = K_2(A_\infty' - A')[\text{Sc}^{3+}]_0 + A_1 \quad (5)$$

where  $A_0'$  and  $A_1$  are the absorbances at 452 nm due to FI in the absence of  $\text{Sc}(\text{OTf})_3$  and due to FI- $\text{Sc}^{3+}$  in the presence of  $\text{Sc}(\text{OTf})_3$ , respectively, and  $A_\infty'$  is the absorbance due to FI- $2\text{Sc}^{3+}$  in the presence of a large excess of  $\text{Sc}(\text{OTf})_3$  such that all FI molecules form the 1:2 complex (FI- $2\text{Sc}^{3+}$ ) with  $\text{Sc}(\text{OTf})_3$ . Since the value of the left-hand side in eq 5 is obtained using the  $K_1$  value, the  $K_2$  value can be determined from the slope of a linear plot between the left-hand side in eq 5 and  $(A_\infty' - A')[\text{Sc}^{3+}]_0$ . Such a linear plot is in Figure 2b, in agreement with eq 5.<sup>30</sup> The  $K_1$  and  $K_2$  values thus obtained for the FI-metal ion complexes are listed in Table 1.

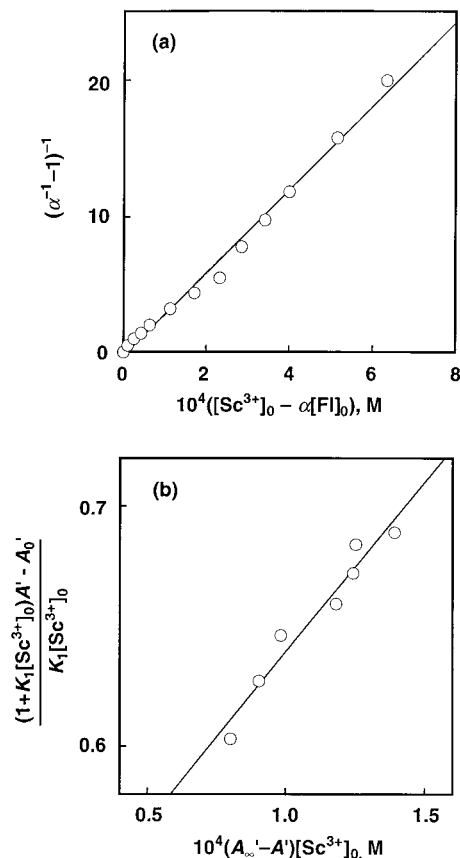


**Figure 2.** Plots for determination of the stepwise complex formation constants (a)  $K_1$  and (b)  $K_2$  for the complex formation of FI ( $1.0 \times 10^{-4}$  M) with  $\text{Sc}^{3+}$  in MeCN.

**TABLE 1: Formation Constants  $K_1$  and  $K_2$  of the FI Complexes with Various Metal Ions,  $\text{Mg}^{2+}$ ,  $\text{Lu}^{3+}$ ,  $\text{Yb}^{3+}$ ,  $\text{La}^{3+}$ , and  $\text{Sc}^{3+}$  in MeCN at 298 K**

	$\text{Mg}^{2+}$	$\text{Lu}^{3+}$	$\text{Yb}^{3+}$	$\text{La}^{3+}$	$\text{Sc}^{3+}$
$K_1, \text{M}^{-1}$	$2.2 \times 10^2$	$4.1 \times 10^2$	$8.8 \times 10^2$	$4.5 \times 10^3$	$3.1 \times 10^4$
$K_2, \text{M}^{-1}$	0.6			$1.6 \times 10^2$	$1.4 \times 10^3$

**TABLE 2: The  $\nu(\text{C}=\text{O})$  Frequencies of the  $\text{C}^2$ - and  $\text{C}^4$ -Carbonyl Groups of FI in the Absence and Presence of  $\text{Sc}^{3+}$ ,  $\text{Yb}^{3+}$  or  $\text{Mg}^{2+}$  Ion in MeCN**

	$\nu(\text{C}^2=\text{O}), \text{cm}^{-1}$	$\nu(\text{C}^4=\text{O}), \text{cm}^{-1}$
none <sup>a</sup>	1689	1718
$[\text{Mg}^{2+}]^b$	1645	1650
$[\text{Yb}^{3+}]^c$	1620	1699
$[\text{Sc}^{3+}]^d$	1606	1677

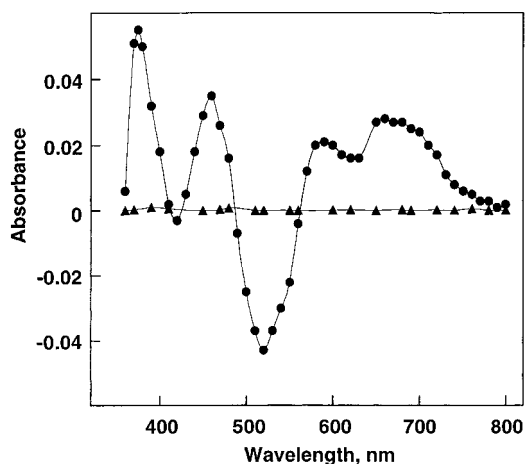
<sup>a</sup> In the absence of metal ion. <sup>b</sup>  $1.0 \times 10^{-1}$  M. <sup>c</sup>  $1.0 \times 10^{-2}$  M. <sup>d</sup>  $3.0 \times 10^{-2}$  M.

The  $K_1$  value increases in order:  $\text{Mg}^{2+} < \text{Lu}^{3+} < \text{Yb}^{3+} < \text{La}^{3+} < \text{Sc}^{3+}$ . The  $K_2$  value increases in the same order, although the  $K_2$  values of the 1:2 complexes of FI with  $\text{Yb}^{3+}$  or  $\text{Lu}^{3+}$  could not be determined because of the low solubility of  $\text{Yb}(\text{OTf})_3$  and  $\text{Lu}(\text{OTf})_3$  in MeCN.

IR spectra of FI in MeCN show three C=O stretching bands assignable to the  $\text{C}^2$ - and  $\text{C}^4$ - and acetate carbonyl groups as reported in the literature.<sup>31</sup> When an excess amount of a metal ion such that most FI molecules form the metal ion complex is added to the MeCN solution of FI, all the C=O stretching bands are significantly red shifted as listed in Table 2. Especially, the C=O stretching band due to the  $\text{C}^2$ -carbonyl group of FI- $2\text{Sc}^{3+}$  is largely red shifted by ca.  $80 \text{ cm}^{-1}$ , suggesting that  $\text{Sc}^{3+}$

**TABLE 3: Fluorescence Maxima ( $\lambda_{\max}$ ), Lifetimes ( $\tau$ ), One-Electron Reduction Potentials ( $E_{\text{red}}^0$ ) of the Singlet Excited States of FI and FI–Metal Ion Complexes and Intrinsic Barriers of Photoinduced Electron Transfer ( $\Delta G^\ddagger_0$ )**

metal ion <sup>a</sup>	$\lambda_{\max}$ , nm	$\tau$ , ns	$E_{\text{red}}^0$ , V vs SCE	$\Delta G^\ddagger_0$ , kcal mol <sup>-1</sup>
none	506	6.5	1.67	3.4
Mg <sup>2+</sup>	504	1.3	2.06	4.0
Yb <sup>3+</sup>	500	0.9	2.25	4.5
Sc <sup>3+</sup>	486	2.4	2.45	4.7

<sup>a</sup> 0.01 M.**Figure 3.** Transient absorption spectra obtained by laser flash photolysis of FI ( $1.0 \times 10^{-5}$  M) in the absence (●) and presence of Yb<sup>3+</sup> (▲,  $1.0 \times 10^{-2}$  M) in deaerated MeCN at 3.0  $\mu$ s after laser excitation at 355 nm.

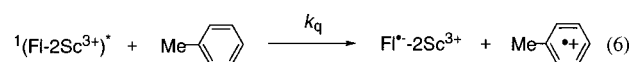
interacts more strongly with C<sup>2</sup>-carbonyl group than the C<sup>4</sup>-carbonyl group.

**Fluorescence Quenching of FI–Metal Ion Complexes.** The complexation of FI with metal ions results in blue shifts of the fluorescence maximum and shortening of the fluorescence lifetime. The fluorescence maxima and the lifetimes of the singlet excited state of FI in the absence and presence of metal ions ( $1.0 \times 10^{-2}$  M) are determined as listed in Table 3. In the case of Sc<sup>3+</sup>, the largest blue shift is observed when FI forms the 1:2 complex (FI–2Sc<sup>3+</sup>) with 0.01 M Sc<sup>3+</sup> (Table 2). The complexation of FI with metal ions also results in the change in the lowest excited state from the  $n, \pi^*$  triplet state to the  $\pi, \pi^*$  singlet state as indicated by the disappearance of the triplet–triplet (T–T) absorption spectrum of FI by the complexation with Yb<sup>3+</sup> (Figure 3). The T–T absorption spectrum of FI in MeCN in Figure 3 shows absorption maxima at  $\lambda = 395, 475, 585,$  and  $655$  nm which agree with the literature values<sup>32</sup> in the absence of metal ions. The T–T absorption spectrum diminishes completely in the presence of Yb(OTf)<sub>3</sub> ( $1.0 \times 10^{-2}$  M) under otherwise the same experimental conditions. Such a change in the lowest excited state may be caused by the complexation of FI with the metal ion. The nonbonding orbital is more stabilized by the complex formation with the metal ion than the  $\pi$ -orbital due to the stronger interaction between nonbonding electrons and the metal ion. On the other hand, the  $\pi, \pi^*$  singlet excited state is more stabilized by the interaction with the metal ion, that is singlet, than the  $\pi, \pi^*$  triplet excited state. Thus, the  $\pi, \pi^*$  excited state in the FI–metal ion complex becomes lower in energy than the  $n, \pi^*$  singlet and triplet excited states in the uncomplexed FI. The change in the lowest excited state from the  $n, \pi^*$  triplet excited state to the  $\pi, \pi^*$  singlet excited state has also been observed when aromatic carbonyl compounds form the complexes with Mg<sup>2+</sup> ion.<sup>13b,33,34</sup>

The observed triplet state quenching in Figure 3 by the metal ion may also be caused by heavy atom quenching.<sup>35</sup> However, the fluorescence intensity and lifetime are changed depending on the metal ion concentration in accordance with the complex formation between FI and the metal ion (vide infra). In the concentration range of Sc<sup>3+</sup> where FI forms a 1:1 complex with Sc<sup>3+</sup>, the fluorescence intensity decreases with increasing Sc<sup>3+</sup> concentration to reach a constant value without change in the fluorescence lifetime (see Supporting Information, S1). The decrease in the fluorescence intensity without change in the lifetime may come from increase in the nonradiative decay rate due to the complex formation between FI and Sc<sup>3+</sup>. The formation constant  $K_1$  ( $3.1 \times 10^4$  M<sup>-1</sup>) determined from the dependence of the initial fluorescence intensity on Sc<sup>3+</sup> concentration (S1) agrees with the value determined from the absorption spectral change in Figure 2a ( $3.1 \times 10^4$  M<sup>-1</sup>).<sup>31</sup> At higher Sc<sup>3+</sup> concentrations, the fluorescence lifetime decreases with increasing Sc<sup>3+</sup> concentration to reach a constant value. The formation constants  $K_1$  and  $K_2$  for 1:1 and 1:2 complexes between FI and Sc<sup>3+</sup> ( $3.2 \times 10^4$  M<sup>-1</sup> and  $1.4 \times 10^3$  M<sup>-1</sup>, respectively) determined from the dependence of the steady-state fluorescence intensity on Sc<sup>3+</sup> concentration (see Supporting Information, S2 and S3) also agree within the experimental error with the values determined from the absorption spectral change in Figures 2a and 2b ( $3.1 \times 10^4$  M<sup>-1</sup> and  $1.4 \times 10^3$  M<sup>-1</sup>, respectively).<sup>30</sup> Such agreement of the  $K_1$  and  $K_2$  values between the fluorescence and absorption spectra confirms that the change in the fluorescence spectrum in the presence of the metal ion is caused by the complex formation between FI and the metal ion.<sup>36</sup>

The fluorescence of FI is quenched via photoinduced electron transfer from electron donors to the singlet excited state (<sup>1</sup>FI\*) in MeCN.<sup>12,37</sup> The effects of metal ions on the oxidizing ability of the singlet excited state of FI are examined by comparing the quenching rate constants ( $k_q$ ) in the presence of a metal ion with those in its absence.

The fluorescence of <sup>1</sup>(FI–2Sc<sup>3+</sup>)\* is efficiently quenched by various electron donors including a relatively weak electron donor such as toluene (eq 6). No fluorescence quenching by



toluene occurs in the case of the FI–Mg<sup>2+</sup> complex or FI in the absence of metal ion. From the slope of the Stern–Volmer plots (eq 1) are obtained quenching constants  $K_q$  ( $= k_q \tau$ ; where  $\tau$  = the fluorescence lifetime) for the fluorescence quenching of FI by alkyl- or methoxy-substituted benzenes in the absence and presence of Sc(OTf)<sub>3</sub>, Yb(OTf)<sub>3</sub>, and Mg(ClO<sub>4</sub>)<sub>2</sub> (see Supporting Information, S4). The  $k_q$  values are listed in Table 4 together with the one-electron oxidation potentials ( $E_{\text{ox}}^0$ ) of the electron donors (see Experimental Section). The quenching rate constants ( $k_q$ ) increase with decreasing the one-electron oxidation potentials of electron donors to reach a diffusion-limited value as shown in Figure 4. This confirms that the fluorescence quenching occurs by photoinduced electron transfer from electron donors to the singlet excited states of FI–metal ion complexes.

The one-electron reduction potential ( $E_{\text{red}}^0$  vs SCE) of the singlet excited state of the FI–metal ion complex can be determined by adaptation of the free energy relationship for photoinduced electron transfer from a series of electron donors to the singlet excited state of the FI–metal ion complex in the presence of a metal ion ( $1.0 \times 10^{-2}$  M) in MeCN at 298 K. The free energy change of photoinduced electron transfer from

**TABLE 4. Quenching Rate Constants ( $k_q$ ) for the Fluorescence Quenching of FI by Alkyl- or Methoxy-Substituted Benzenes and the One-Electron Oxidation Potentials ( $E_{ox}^0$ ) in the Absence and Presence of  $1.0 \times 10^{-2}$  M Metal Ions in MeCN**

no.	substituted benzene	$E_{ox}^0,^a$ V vs SCE	$k_q, M^{-1} s^{-1}$ in the presence of			
			Sc <sup>3+</sup>	Yb <sup>3+</sup>	Mg <sup>2+</sup>	none <sup>b</sup>
1	toluene	2.20	$1.0 \times 10^9$	$1.3 \times 10^8$	<i>c</i>	<i>c</i>
2	ethylbenzene	2.14	$1.5 \times 10^9$	$3.8 \times 10^8$	<i>c</i>	<i>c</i>
3	<i>m</i> -xylene	2.02	$3.8 \times 10^9$		$6.3 \times 10^8$	<i>c</i>
4	<i>o</i> -xylene	1.98	$4.8 \times 10^9$	$1.9 \times 10^9$	$7.0 \times 10^8$	<i>c</i>
5	<i>p</i> -cymene	1.96	$4.4 \times 10^9$		$1.3 \times 10^9$	<i>c</i>
6	<i>p</i> -xylene	1.93	$5.7 \times 10^9$	$2.6 \times 10^9$	$1.4 \times 10^9$	<i>c</i>
7	1,2,3-trimethylbenzene	1.88	$5.5 \times 10^9$	$2.8 \times 10^9$	$1.8 \times 10^9$	<i>c</i>
8	1,2,4-trimethylbenzene	1.79	$6.5 \times 10^9$	$4.1 \times 10^9$	$2.3 \times 10^9$	<i>c</i>
9	1,2,3,5-tetramethylbenzene	1.71	$7.6 \times 10^9$		$4.2 \times 10^9$	$1.2 \times 10^8$
10	1,2,3,4-tetramethylbenzene	1.71	$7.8 \times 10^9$	$6.4 \times 10^9$		$1.5 \times 10^8$
11	pentamethylbenzene	1.58		$9.3 \times 10^9$	$1.3 \times 10^{10}$	$1.3 \times 10^9$
12	<i>m</i> -dimethoxybenzene	1.50	$1.1 \times 10^{10}$			$3.2 \times 10^9$

<sup>a</sup> Determined using the SHACV method in MeCN containing 0.1 M TBAP. <sup>b</sup> In the absence of metal ion. <sup>c</sup> Too small to be determined accurately.

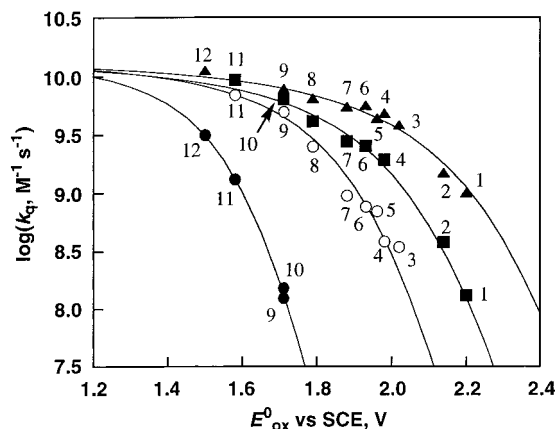


**Figure 4.** Plots of the logarithm of the quenching rate constant ( $k_q$ ) for the fluorescence quenching of FI ( $1.0 \times 10^{-5}$  M) in the absence (●) and presence of Sc<sup>3+</sup> (▲), Yb<sup>3+</sup> (■), and Mg<sup>2+</sup> (○) ( $1.0 \times 10^{-2}$  M) by substituted benzenes: toluene (1), ethylbenzene (2), *m*-xylene (3), *o*-xylene (4), *p*-cymene (5), *p*-xylene (6), 1,2,3-trimethylbenzene (7), 1,2,4-trimethylbenzene (8), 1,2,3,4-tetramethylbenzene (9), 1,2,3,5-tetramethylbenzene (10), pentamethylbenzene (11), and *m*-dimethoxybenzene (12) vs one-electron oxidation potential ( $E_{ox}^0$ ) of the substituted benzenes in MeCN at 298 K.

electron donors to the singlet excited state of the FI–metal ion complex ( $\Delta G_{et}^0$ ) is given by eq 7,

$$\Delta G_{et}^0 = e(E_{ox}^0 - E_{red}^{0*}) \quad (7)$$

where  $e$  is the elementary charge, and  $E_{ox}^0$  is the one-electron oxidation potential of an electron donor. The dependence of the activation free energy of photoinduced electron transfer ( $\Delta G_{et}^\ddagger$ ) on the free energy change of electron transfer ( $\Delta G_{et}^0$ ) has well been established as given by the free energy relationship (eq 8),<sup>38</sup>

$$\Delta G_{et}^\ddagger = (\Delta G_{et}^0/2) + [(\Delta G_{et}^0/2)^2 + (\Delta G_{et}^\ddagger_0)^2]^{1/2} \quad (8)$$

where  $\Delta G_{et}^\ddagger_0$  is the intrinsic barrier that represents the activation free energy when the driving force of electron transfer is zero, i.e.,  $\Delta G_{et}^\ddagger = \Delta G_{et}^\ddagger_0$  at  $\Delta G_{et}^0 = 0$ . On the other hand, the  $\Delta G_{et}^\ddagger$  values are related to the fluorescence quenching rate constant ( $k_q$ ) for the photoinduced electron transfer as given by eq 9,

$$\Delta G_{et}^\ddagger = 2.3k_B T \log[Z(k_q^{-1} - k_{diff}^{-1})] \quad (9)$$

where  $k_B$  is the Boltzmann constant,  $Z$  is the collision frequency that is taken as  $1 \times 10^{11} M^{-1} s^{-1}$ , and  $k_{diff}$  is the diffusion rate constant ( $2.0 \times 10^{10} M^{-1} s^{-1}$ ) in MeCN.<sup>38</sup>

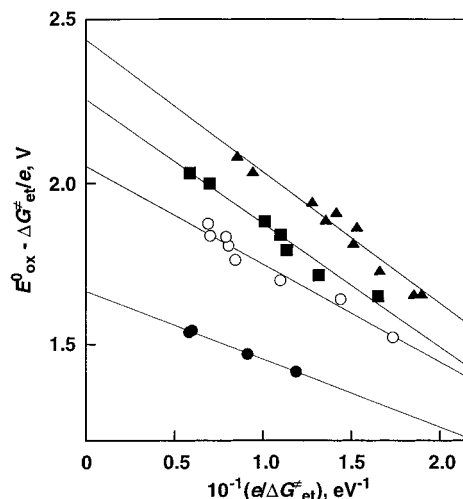


**Figure 5.** Plots of  $E_{ox}^0 - (\Delta G_{et}^\ddagger/e)$  vs  $(e/\Delta G_{et}^\ddagger)$  for the data in Figure 4.

From eqs 7 and 8 is derived a linear relationship between  $E_{ox}^0 - (\Delta G_{et}^\ddagger/e)$  and  $(e/\Delta G_{et}^\ddagger)$  as given by eq 10.<sup>39</sup>

$$E_{ox}^0 - (\Delta G_{et}^\ddagger/e) = E_{red}^{0*} - (\Delta G_{et}^\ddagger_0/e)^2 / (\Delta G_{et}^\ddagger/e) \quad (10)$$

The  $\Delta G_{et}^\ddagger$  values are obtained from the  $k_q$  values using eq 9. Thus, the unknown values of  $E_{red}^{0*}$  and  $\Delta G_{et}^\ddagger_0$  can be determined from the intercept and slope of the linear plots of  $E_{ox}^0 - (\Delta G_{et}^\ddagger/e)$  vs  $(e/\Delta G_{et}^\ddagger)$  as shown in Figure 5. The order of  $E_{red}^{0*}$  (vs SCE) values of FI–metal ion complexes is  ${}^1(\text{FI}-2\text{Sc}^{3+})^*$  (2.45 V) >  ${}^1(\text{FI}-\text{Yb}^{3+})^*$  (2.25 V) >  ${}^1(\text{FI}-\text{Mg}^{2+})^*$  (2.06 V) >  ${}^1\text{FI}^*$  (1.67 V), and this order is consistent with that of the formation constants ( $K_1$ ) of FI–metal ion complexes.<sup>40</sup> The comparison of the  $E_{red}^{0*}$  value of  ${}^1(\text{FI}-2\text{Sc}^{3+})^*$  with that of  ${}^1\text{FI}^*$  reveals the remarkable positive shifts (ca. 780 mV) of the  $E_{red}^{0*}$  value of  ${}^1(\text{FI}-2\text{Sc}^{3+})^*$  as compared to that of  ${}^1\text{FI}^*$ . Such a large positive shift of the  $E_{red}^{0*}$  value results in a significant increase in the reactivity of  ${}^1(\text{FI}-2\text{Sc}^{3+})^*$  vs uncomplexed FI in the photoinduced electron-transfer reactions in Figure 5.

**Photooxidation of *p*-Chlorobenzyl Alcohol by FI–2Sc<sup>3+</sup>.** The remarkable enhancement of the redox reactivity of  ${}^1(\text{FI}-2\text{Sc}^{3+})^*$  as compared to that of  ${}^1\text{FI}^*$  and  ${}^1(\text{FI}-\text{Mg}^{2+})^*$  makes it possible to oxidize efficiently *p*-chlorobenzyl alcohol by  ${}^1(\text{FI}-2\text{Sc}^{3+})^*$ . Irradiation of a deaerated MeCN solution containing FI, *p*-chlorobenzyl alcohol, and Sc(OTf)<sub>3</sub> with visible light at  $\lambda > 420$  nm results in the formation of *p*-chlorobenzaldehyde and FIH<sub>2</sub> (eq 11). No photooxidation of *p*-chlorobenzyl alcohol was observed in the absence of the metal ion under otherwise

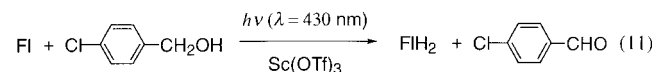
**TABLE 5: Quantum Yields ( $\Phi$ ) of the Photooxidation of *p*-Chloro- and Methoxybenzyl Alcohol by FI–Metal Ion Complexes in Deaerated MeCN at 298 K**

metal ion <sup>a</sup>	$\Phi(p\text{-ClC}_6\text{H}_4\text{CH}_2\text{OH})^b$	$\Phi(p\text{-MeOC}_6\text{H}_4\text{CH}_2\text{OH})^c$
Sc <sup>3+</sup>	$1.7 \times 10^{-1}$	$1.2 \times 10^{-1}$
La <sup>3+</sup>	$2.4 \times 10^{-2}$	$5.7 \times 10^{-2}$
Lu <sup>3+</sup>	$6.2 \times 10^{-3}$	$1.7 \times 10^{-1}$
Yb <sup>3+</sup>	$3.3 \times 10^{-3}$	$6.0 \times 10^{-3}$
Mg <sup>2+</sup>	$1.9 \times 10^{-3}$	$6.6 \times 10^{-2}$

<sup>a</sup> Metal ion is used as a triflate salt; [metal ion] =  $1.0 \times 10^{-2}$  M.

<sup>b</sup> [FI] =  $2.0 \times 10^{-4}$  M, [*p*-ClC<sub>6</sub>H<sub>4</sub>CH<sub>2</sub>OH] =  $8.0 \times 10^{-1}$  M. <sup>c</sup> [FI] =  $3.0 \times 10^{-4}$  M, [*p*-MeOC<sub>6</sub>H<sub>4</sub>CH<sub>2</sub>OH] =  $2.7 \times 10^{-2}$  M.

the same experimental conditions. Similarly, the photooxidation of *p*-chlorobenzyl alcohol by FI proceeds in the presence of other metal triflates such as La(OTf)<sub>3</sub>, Lu(OTf)<sub>3</sub>, Sc(OTf)<sub>3</sub>, and



Mg(OTf)<sub>2</sub>. The quantum yields ( $\Phi$ ) for the photooxidation of *p*-chlorobenzyl alcohol ( $8.0 \times 10^{-1}$  M) in the presence of FI ( $2.0 \times 10^{-4}$  M) and metal triflates ( $1.0 \times 10^{-2}$  M) were determined from the rate of disappearance of the absorption band due to the FI–metal ion complexes under irradiation of monochromatized light of  $\lambda = 430$  nm (see Supporting Information, S5). In the presence of  $1.0 \times 10^{-2}$  M metal ion, FI forms the 1:2 complex with Sc<sup>3+</sup> and La<sup>3+</sup> and the 1:1 complex with other metal ions (Table 1). The  $\Phi$  values are listed in Table 5. The  $\Phi$  value is largest in the case of Sc(OTf)<sub>3</sub> ( $\Phi = 0.17$ ) and decreases in order: Sc<sup>3+</sup> > La<sup>3+</sup> > Lu<sup>3+</sup> > Yb<sup>3+</sup> > Mg<sup>2+</sup>. When *p*-chlorobenzyl alcohol is replaced by *p*-methoxybenzyl alcohol that is a stronger electron donor, the  $\Phi$  values of FI–metal ion complexes become larger except for the case of Sc(OTf)<sub>3</sub> (Table 5).

The  $\Phi$  value for the photooxidation of *p*-chlorobenzyl alcohol to *p*-chlorobenzaldehyde in MeCN increases with an increase in the concentration of *p*-chlorobenzyl alcohol [*p*-ClC<sub>6</sub>H<sub>4</sub>CH<sub>2</sub>OH] to approach a limiting value ( $\Phi_\infty$ ) as shown in Figure 6a. The dependence of quantum yields on [*p*-ClC<sub>6</sub>H<sub>4</sub>CH<sub>2</sub>OH] is expressed by eq 12,

$$\Phi = \Phi_\infty K_{\text{obs}} [p\text{-ClC}_6\text{H}_4\text{CH}_2\text{OH}] / (1 + K_{\text{obs}} [p\text{-ClC}_6\text{H}_4\text{CH}_2\text{OH}]) \quad (12)$$

which is rewritten as a linear correlation between  $\Phi^{-1}$  vs [*p*-ClC<sub>6</sub>H<sub>4</sub>CH<sub>2</sub>OH]<sup>-1</sup> (eq 13),

$$\Phi^{-1} = \Phi_\infty^{-1} [1 + (K_{\text{obs}} [p\text{-ClC}_6\text{H}_4\text{CH}_2\text{OH}])^{-1}] \quad (13)$$

where  $K_{\text{obs}}$  is the quenching constant of <sup>1</sup>(FI–2Sc<sup>3+</sup>)\* by *p*-ClC<sub>6</sub>H<sub>4</sub>CH<sub>2</sub>OH. The validity of eq 13 is confirmed by the plot of  $\Phi^{-1}$  vs [*p*-ClC<sub>6</sub>H<sub>4</sub>CH<sub>2</sub>OH]<sup>-1</sup> as shown in Figure 6b. From the slope and the intercept are obtained the values of  $\Phi_\infty$  ( $2.3 \times 10^{-1}$ ) and  $K_{\text{obs}}$  ( $4.0 \text{ M}^{-1}$ ). The quenching constant  $K_{\text{obs}}$  (=  $k_{\text{obs}}\tau$ ) is converted to the rate constant ( $k_{\text{obs}} = 1.6 \times 10^9 \text{ M}^{-1} \text{ s}^{-1}$ ) of the reaction of <sup>1</sup>(FI–2Sc<sup>3+</sup>)\* with *p*-chlorobenzyl alcohol using the fluorescence lifetime (2.4 ns). Since the one-electron oxidation potential of *p*-chlorobenzyl alcohol ( $E_{\text{ox}}^0$  vs SCE in MeCN = 1.88 V)<sup>41</sup> lies within the range of the oxidation potentials of substituted benzenes used for the fluorescence quenching of <sup>1</sup>(FI–2Sc<sup>3+</sup>)\* via electron transfer (Table 4), fluorescence quenching of <sup>1</sup>(FI–2Sc<sup>3+</sup>)\* by *p*-chlorobenzyl alcohol also occurred efficiently. The fluorescence quenching rate constant ( $k_q$ ) of <sup>1</sup>(FI–2Sc<sup>3+</sup>)\* by *p*-chlorobenzyl alcohol

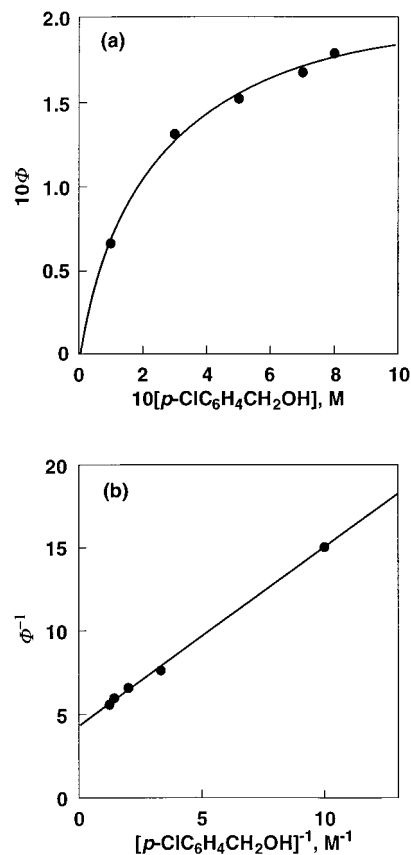


**Figure 6.** (a) Dependence of the quantum yield ( $\Phi$ ) on [*p*-ClC<sub>6</sub>H<sub>4</sub>CH<sub>2</sub>OH] for the photoreduction of FI ( $1.5 \times 10^{-4}$  M) with *p*-ClC<sub>6</sub>H<sub>4</sub>CH<sub>2</sub>OH in the presence of Sc<sup>3+</sup> ( $1.0 \times 10^{-2}$  M) in deaerated MeCN at 298 K. (b) Plot of  $\Phi^{-1}$  vs [*p*-ClC<sub>6</sub>H<sub>4</sub>CH<sub>2</sub>OH]<sup>-1</sup>.

was obtained from the Stern–Volmer relationship (vide supra). The  $k_q$  value thus obtained is  $1.8 \times 10^9 \text{ M}^{-1} \text{ s}^{-1}$  which agrees with the  $k_{\text{obs}}$  value. Such an agreement indicates that the photooxidation of *p*-chlorobenzyl alcohol by FI in the presence of Sc(OTf)<sub>3</sub> proceeds via electron transfer from *p*-chlorobenzyl alcohol to <sup>1</sup>(FI–2Sc<sup>3+</sup>)\* which has much stronger oxidizing ability than <sup>1</sup>FI\*.

The occurrence of photoinduced electron transfer in the photooxidation of *p*-chlorobenzyl alcohol by FI–2Sc<sup>3+</sup> has been confirmed by the laser flash photolysis study as follows. The transient absorption spectra in the visible region ( $\lambda_{\text{max}} = 560$  nm) are observed by the laser flash photolysis of a deaerated MeCN solution containing FI, Sc(OTf)<sub>3</sub>, and *p*-chlorobenzyl alcohol with 440 nm laser light as shown in Figure 7a. To assign the absorption bands in Figure 7a, FI\*–2Sc<sup>3+</sup> was produced by electron transfer from a dimeric 1-benzyl-1,4-dihydronicotinamide [(BNA)<sub>2</sub>]<sup>42</sup> to FI in the presence of Sc(OTf)<sub>3</sub> in MeCN. The (BNA)<sub>2</sub> is known to act as a unique two-electron donor to produce two equivalents of the radical anions of electron acceptors.<sup>42–44</sup> The absorption spectrum due to FI\*–2Sc<sup>3+</sup> is shown in Figure 7b, where the absorption band at 510 nm is red shifted as compared to the reported band of the radical anion of *N*(10)-isobutyl-*N*(3)-methyl flavin ( $\lambda_{\text{max}} = 478$  nm).<sup>45</sup>

The formation of FI\*–2Sc<sup>3+</sup> is confirmed by the ESR spectrum as shown in Figure 8a which exhibits apparent 13 line signals centered at  $g = 2.0033$ . The hyperfine coupling constants are determined as given in Figure 8b by the computer simulation of the ESR spectrum. A similar but slightly different ESR spectrum was obtained for FI\* which was produced by photoinduced electron transfer from (BNA)<sub>2</sub> to FI in the absence of Sc<sup>3+</sup> ion in MeCN (see Supporting Information, S6). The

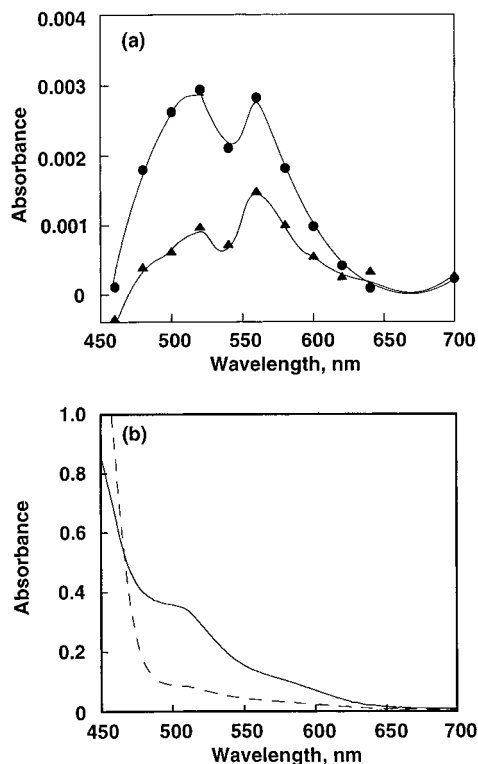
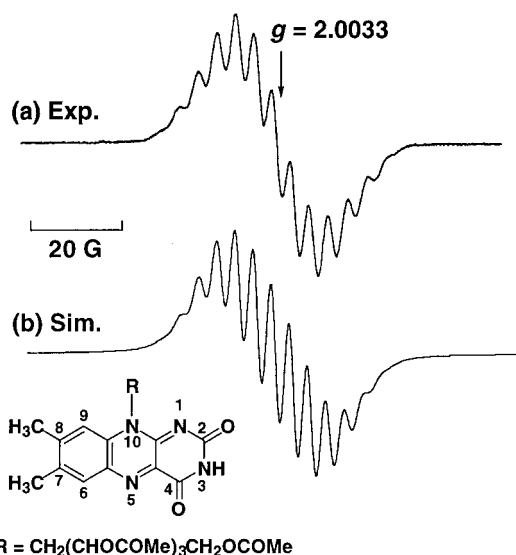


**Figure 7.** (a) Transient absorption spectra observed in the photochemical reaction of the FI-2Sc(OTf)<sub>3</sub> complex formed between FI ( $1.0 \times 10^{-4}$  M) and Sc(OTf)<sub>3</sub> ( $1.0 \times 10^{-2}$  M) with *p*-ClC<sub>6</sub>H<sub>4</sub>CH<sub>2</sub>OH (1.0 M) at 25  $\mu$ s (●) and 250  $\mu$ s (▲) after laser excitation in deaerated MeCN at 298 K. (b) Visible spectra observed in the electron-transfer reduction of FI ( $1.0 \times 10^{-4}$  M) by (BNA)<sub>2</sub> ( $1.0 \times 10^{-3}$  M) in the presence of Sc(OTf)<sub>3</sub> ( $3.0 \times 10^{-3}$  M) at 5 s (broken line) and 120 s (solid line) in deaerated MeCN at 298 K.

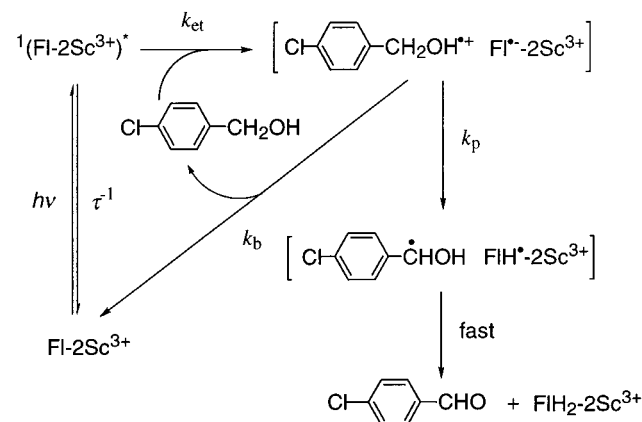


R = CH<sub>2</sub>(CHOCOMe)<sub>2</sub>CH<sub>2</sub>OCOMe

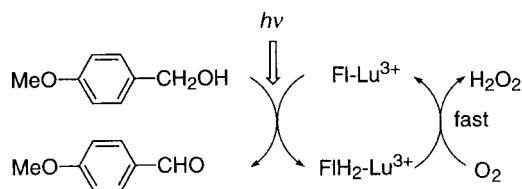
**Figure 8.** (a) ESR spectrum of FI<sup>•-</sup>-2Sc<sup>3+</sup> generated in the photo-induced reaction of FI ( $3.0 \times 10^{-3}$  M) with (BNA)<sub>2</sub> ( $6.0 \times 10^{-3}$  M) and Sc(OTf)<sub>3</sub> ( $1.0 \times 10^{-2}$  M) in deaerated MeCN at 298 K. (b) Computer simulation spectrum with  $g = 2.0033$ ,  $a(\text{N}^5) = 7.2$  G,  $a(\text{N}^{10}) = 3.8$  G,  $a(\text{H}^6) = 3.6$  G,  $a(3\text{H}^7) = 0.7$  G,  $a(3\text{H}^8) = 3.6$  G,  $a(\text{N}^{10}-\text{CH}_2) = 3.8$  G,  $\Delta H_{\text{msl}} = 2.2$  G. The spin densities of the radical anion of *N*(10)-methyl flavin calculated using density functional theory at the Becke3LYP/6-311++G\*\* level are 0.378 (N<sup>5</sup>), 0.077 (N<sup>10</sup>), 0.186 (C<sup>6</sup>), -0.104 (C<sup>7</sup>), 0.201 (C<sup>8</sup>), 0.039 (C<sup>2=O</sup>), 0.0628 (C<sup>4=O</sup>).

ESR spectrum of FI<sup>•-</sup> is essentially the same as that reported for the radical anion of *N*(10)-isobutyl-*N*(3)-methyl flavin which exhibits apparent 12 line signals centered at  $g = 2.0038$ .<sup>45</sup> The

### SCHEME 1



### SCHEME 2



spin densities of the radical anion of *N*(10)-methyl flavin were calculated using density functional theory at the Becke3LYP/6-311++G\*\* level (see Experimental Section) as shown in Figure 8b.<sup>46,47</sup> Since there is essentially no spin density on the carbonyl oxygens which can bind with Sc<sup>3+</sup>, the ESR spectrum of FI<sup>•-</sup>-2Sc<sup>3+</sup> is only slightly different from that of FI<sup>•-</sup>.

The transient absorption spectra in Figure 7a ( $\lambda_{\text{max}} = 560$  nm) are clearly different from that of FI<sup>•-</sup>-2Sc<sup>3+</sup> ( $\lambda_{\text{max}} = 510$  nm) or FI<sup>•-</sup> ( $\lambda_{\text{max}} = 478$  nm). The absorption bands in the long wavelength region between 500 and 600 nm are rather similar to those reported for the neutral radical (FIH<sup>•</sup>).<sup>32a</sup> Thus, the transient absorption band at  $\lambda_{\text{max}} = 560$  nm in Figure 7a may be assigned due to FIH<sup>•</sup>-2Sc<sup>3+</sup> which is produced by proton transfer from *p*-ClC<sub>6</sub>H<sub>4</sub>CH<sub>2</sub>OH<sup>•+</sup> to FI<sup>•-</sup>-2Sc<sup>3+</sup>. The absorption band at 520 nm observed at 25  $\mu$ s after the laser excitation may be overlapped with that due to FI<sup>•-</sup>-2Sc<sup>3+</sup> ( $\lambda_{\text{max}} = 510$  nm).

On the basis of the results and discussion described above, the reaction mechanism of photooxidation of *p*-chlorobenzyl alcohol by FI-2Sc<sup>3+</sup> is summarized as shown in Scheme 1. The singlet excited state <sup>1</sup>(FI-2Sc<sup>3+</sup>)\* is quenched by electron transfer from *p*-chlorobenzyl alcohol ( $k_{\text{et}}$ ) to give the radical ion pair [*p*-ClC<sub>6</sub>H<sub>4</sub>CH<sub>2</sub>OH<sup>•+</sup> FI<sup>•-</sup>-2Sc<sup>3+</sup>] in competition with the decay to the ground state. Then, a proton is transferred from *p*-chlorobenzyl alcohol radical cation to FI<sup>•-</sup>-2Sc<sup>3+</sup> in the radical ion pair to give the radical pair [*p*-ClC<sub>6</sub>H<sub>4</sub>CHOH<sup>•</sup> FIH<sup>•</sup>-2Sc<sup>3+</sup>] as observed in the transient spectra in Figure 7a.<sup>48</sup> The hydrogen transfer from *p*-ClC<sub>6</sub>H<sub>4</sub>CHOH<sup>•</sup> to FIH<sup>•</sup>-2Sc<sup>3+</sup> yields the product *p*-ClC<sub>6</sub>H<sub>4</sub>CHO and FIH<sub>2</sub>-2Sc<sup>3+</sup>.<sup>12</sup> The proton-transfer step ( $k_{\text{p}}$ ) may compete well with the back electron-transfer step to the reactant pair ( $k_{\text{b}}$ ).

By applying the steady-state approximation to the reactive species, <sup>1</sup>(FI-2Sc<sup>3+</sup>)\* and the radical ion and radical pairs in Scheme 2, the dependence of  $\Phi$  on the *p*-chlorobenzyl alcohol concentration [*p*-ClC<sub>6</sub>H<sub>4</sub>CH<sub>2</sub>OH] can be derived as given by eq 14,

$$\Phi = \frac{[k_{\text{p}}/(k_{\text{p}} + k_{\text{b}})]k_{\text{et}}\tau[p\text{-ClC}_6\text{H}_4\text{CH}_2\text{OH}]}{(1 + k_{\text{et}}\tau[p\text{-ClC}_6\text{H}_4\text{CH}_2\text{OH}])} \quad (14)$$



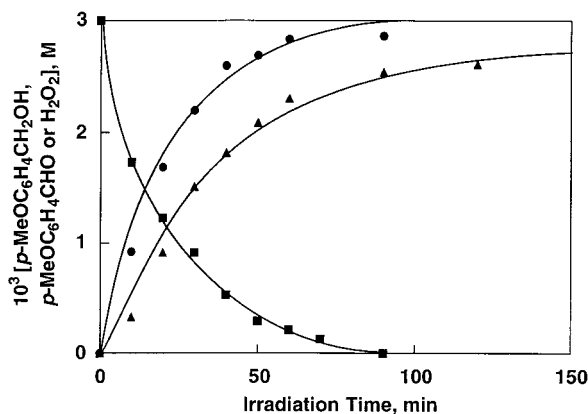
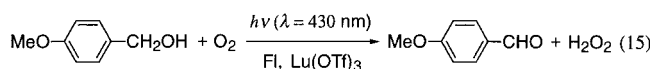


**Figure 9.** Time dependence of the concentration of *p*-MeOC<sub>6</sub>H<sub>4</sub>CH<sub>2</sub>OH (■), *p*-MeOC<sub>6</sub>H<sub>4</sub>CHO (●), and H<sub>2</sub>O<sub>2</sub> (▲) for the photooxidation of *p*-MeOC<sub>6</sub>H<sub>4</sub>CH<sub>2</sub>OH (3.0 × 10<sup>-3</sup> M) with oxygen catalyzed by Fl (2.0 × 10<sup>-4</sup> M) in the presence of Lu<sup>3+</sup> (1.0 × 10<sup>-2</sup> M) under visible light irradiation (λ = 430 nm) in MeCN at 298 K.

which agrees with the observed dependence of Φ on [*p*-ClC<sub>6</sub>H<sub>4</sub>CH<sub>2</sub>OH] in eq 12. The limiting quantum yield Φ<sub>∞</sub> corresponds to  $k_p/(k_p + k_b)$ . Thus, the Φ<sub>∞</sub> values being smaller than unity may be ascribed to the competition of the proton-transfer process ( $k_p$ ) with the back electron-transfer process ( $k_b$ ).

**Photocatalytic Oxidation of *p*-Methoxybenzyl Alcohol by Oxygen.** Since the Fl–Lu<sup>3+</sup> complex gives the largest Φ value (0.17) for the photooxidation of *p*-methoxybenzyl alcohol in deaerated MeCN (Table 5), the photocatalytic oxidation of *p*-methoxybenzyl alcohol by oxygen is examined using the Fl–Lu<sup>3+</sup> complex. When an oxygen-saturated MeCN solution containing *p*-methoxybenzyl alcohol (3.0 × 10<sup>-3</sup> M), Lu(OTf)<sub>3</sub> (1.0 × 10<sup>-2</sup> M) and the catalytic amount of Fl (2.0 × 10<sup>-4</sup> M) was irradiated with visible monochromatized light (λ = 430 nm), the decrease in the concentration of *p*-methoxybenzyl alcohol was accompanied by the increase in the concentration of *p*-methoxybenzaldehyde and H<sub>2</sub>O<sub>2</sub> (eq 15). Yields of *p*-



methoxybenzaldehyde based on the initial amount of Fl exceed 1400% in 50 min irradiation, demonstrating an efficient recycling of Fl in the photooxidation of *p*-methoxybenzyl alcohol as shown in Figure 9. Thus, Fl acts as an efficient photocatalyst for the oxidation of *p*-methoxybenzyl alcohol in the presence of Lu(OTf)<sub>3</sub> and oxygen. The disappearance of *p*-methoxybenzyl alcohol coincides well with the formation of *p*-methoxybenzaldehyde. The amount of H<sub>2</sub>O<sub>2</sub> formed by the photooxidation of *p*-methoxybenzyl alcohol is somewhat smaller than that of *p*-methoxybenzaldehyde due to the partial decomposition of H<sub>2</sub>O<sub>2</sub> during the photochemical reaction. In contrast with the efficient photocatalysis in the presence of Lu(OTf)<sub>3</sub>, the photodegradation of photocatalyst (Fl) occurs in the presence of Mg(OTf)<sub>2</sub> and the yields of H<sub>2</sub>O<sub>2</sub> as well as *p*-methoxybenzaldehyde become much lower than those in the presence of Lu(OTf)<sub>3</sub>. In this case, Lu(OTf)<sub>3</sub> can not only act as an efficient co-catalyst in the photooxidation of *p*-methoxybenzyl alcohol catalyzed by Fl but also prevents Fl from the photodegradation.

The quantum yield (Φ) of the photocatalytic oxidation of *p*-methoxybenzyl alcohol by oxygen in the presence of Fl–Lu<sup>3+</sup> was determined from the rate of formation of *p*-methoxybenzaldehyde (see Experimental Section). The Φ value for the photooxidation of *p*-methoxybenzyl alcohol by Fl–Lu<sup>3+</sup> in oxygen-saturated MeCN increases with increasing the concen-

tration of *p*-methoxybenzyl alcohol to reach a constant value Φ<sub>∞</sub> = 0.17 at [*p*-MeOC<sub>6</sub>H<sub>4</sub>CH<sub>2</sub>OH] = 2.7 × 10<sup>-2</sup> M, which agrees with the corresponding value (0.17) for the photooxidation of *p*-methoxybenzyl alcohol by Fl–Lu<sup>3+</sup> in deaerated MeCN (Table 5). Such an agreement indicates that oxidation of the reduced flavin, FlH<sub>2</sub>–Lu<sup>3+</sup>, by oxygen to regenerate Fl–Lu<sup>3+</sup> is too fast to affect the Φ value as shown in Scheme 2. The rare-earth metal ion may accelerate the oxidation of the reduced flavin by oxygen to yield H<sub>2</sub>O<sub>2</sub> as reported for the Mg<sup>2+</sup>-catalyzed oxidation of reduced flavin by oxygen.<sup>49</sup> Although the triplet excited state of Fl is quenched by oxygen that is a well-known triplet quencher,<sup>50</sup> the Fl–metal ion complexes can act as efficient and stable photocatalysts in the photooxidation of benzyl alcohol derivatives by oxygen due to the change in the spin state from the n,π\* triplet to the π,π\* singlet excited state by the complexation with metal ions (Figure 3).

**Acknowledgment.** We are grateful to Dr. A. Ishida for the measurements of laser flash photolysis at the early stage of this study. This work was partially supported by a Grant-in-Aid for Scientific Research Priority Area (Nos. 11228205 and 413/13031059) from the Ministry of Education, Culture, Sports, Science and Technology, Japan.

**Supporting Information Available:** Change in the fluorescence decay curve of Fl with Sc<sup>3+</sup> concentration (S1), change in the steady-state fluorescence spectra on Sc<sup>3+</sup> concentration (S2,S3), Stern–Volmer plots for the fluorescence quenching of Fl by various alkylbenzenes in the presence of Sc<sup>3+</sup> (S4); electronic spectra observed in the photochemical reaction of Fl with *p*-ClC<sub>6</sub>H<sub>4</sub>CH<sub>2</sub>OH in the presence of Sc<sup>3+</sup> (S5); ESR spectrum of Fl<sup>•-</sup> generated in photoinduced electron transfer from (BNA)<sub>2</sub> to Fl, and the computer simulation spectrum (S6). This material is available free of charge via the Internet at <http://pubs.acs.org>.

## References and Notes

- (1) (a) Tollin, G. In *Electron Transfer in Chemistry*; Balzani, V., Ed.; Wiley-VCH: Weinheim, 2001; Vol. 5, pp 202–231. (b) *Chemistry and Biochemistry of Flavoenzymes*; Müller, F., Ed.; CRC: Boca Raton, FL, 1991; Vols. 1–3.
- (2) (a) Sanner, C.; Macheroux, P.; Rueterjans, H.; Müller, F.; Bacher, A. *Eur. J. Biochem.* **1991**, *196*, 663. (b) Breinlinger, E. C.; Rotello, V. M. *J. Am. Chem. Soc.* **1997**, *119*, 1165. (c) Greaves, M. D.; Rotello, V. M. *J. Am. Chem. Soc.* **1997**, *119*, 10569. (d) Deans, R.; Cook, G.; Rotello, V. M. *J. Org. Chem.* **1997**, *62*, 836. (e) Fox, K.; Karplus, P. *J. Biol. Chem.* **1999**, *274*, 9357. (f) Kajiki, T.; Moriya, H.; Kondo, S.; Nabeshima, T.; Yano, Y. *J. Chem. Soc., Chem. Commun.* **1998**, 2727. (g) Cuello, A. O.; McIntosh, C. M.; Rotello, V. M. *J. Am. Chem. Soc.* **2000**, *122*, 3517.
- (3) (a) Breinlinger, E. C.; Niemz, A.; Rotello, V. M. *J. Am. Chem. Soc.* **1995**, *117*, 5379. (b) Swenson, R. P.; Krey, G. D. *Biochemistry* **1994**, *33*, 8505. (c) Palfey, B. A.; Moran, G. R.; Entsch, B.; Ballou, D. P.; Massey, V. *Biochemistry* **1999**, *38*, 1153.
- (4) Breinlinger, E. C.; Keenan, C. J.; Rotello, V. M. *J. Am. Chem. Soc.* **1998**, *120*, 8606.
- (5) Hasford, J. J.; Kemnitzer, W.; Rizzo, C. J. *J. Org. Chem.* **1997**, *62*, 5244.
- (6) (a) Hemmerich, P.; Lauterwein, J. In *The Structure and Reactivity of Flavin-Metal Complexes, in Inorganic Biochemistry*; Eichhorn, G. L., Ed.; Elsevier: Amsterdam, 1973; p 1168. (b) Clarke, M. J. *Comments Inorg. Chem.* **1984**, *3*, 133.
- (7) (a) Niemz, A.; Rotello, V. M. *Acc. Chem. Res.* **1999**, *32*, 44. (b) Rotello, V. M. In *Electron Transfer in Chemistry*; Balzani, V., Ed.; Wiley-VCH: Weinheim, 2001; Vol. 4, pp 68–87.
- (8) (a) Cadet, J.; Vigny, P. In *Bioorganic Photochemistry*; Morrison, H., Ed.; Wiley: New York, 1990; Vol. 1, pp 1–272. (b) Heelis, P. F. In *Chemistry and Biochemistry of Flavoenzymes*; Müller, F., Ed.; CRC Press: Boca Raton, FL, 1991; Vol. 1, pp 171–193. (c) Penzer, G. R.; Radda, G. K. In *Methods in Enzymology*; McCormick, D. B., Wright, L. D., Eds.; Academic Press: New York, 1971; Vol. XVIII, p 479. (d) Fukuzumi, S.;

- Tanaka, T. In *Photoinduced Electron Transfer*; Fox, M. A., Chanon, M., Eds.; Elsevier: Amsterdam, 1988; Part C, pp 636–687.
- (9) (a) Novak, M.; Miller, A.; Bruce, T. C.; Tollin, G. *J. Am. Chem. Soc.* **1980**, *102*, 1465. (b) Pac, C.; Miyake, K.; Masaki, Y.; Yanagida, S.; Ohno, T.; Yoshimura, A. *J. Am. Chem. Soc.* **1992**, *114*, 10756. (c) Hearst, J. E. *Science* **1995**, *268*, 1858. (d) Kasai, H.; Yamaizumi, Z.; Berger, M.; Cadet, J. *J. Am. Chem. Soc.* **1992**, *114*, 9692. (e) Epple, R.; Wallenborn, E.-U.; Carell, T. *J. Am. Chem. Soc.* **1997**, *119*, 7440.
- (10) (a) Traber, R.; Werner, T.; Schreiner, S.; Kramer, H. E. A.; Knappe, W.-R.; Hemmerich, P. In *Flavins and Flavoproteins*; Yagi, K., Yamano, T., Eds.; Japan Scientific Society Press: Tokyo, 1980; p 431. (b) Heelis, P. F. *Chem. Soc. Rev.* **1982**, *11*, 15. (c) Müller, F. *Photochem. Photobiol.* **1981**, *34*, 753.
- (11) (a) Fukuzumi, S. *Bull. Chem. Soc. Jpn.* **1997**, *70*, 1. (b) Fukuzumi, S.; Kuroda, S.; Tanaka, T. *J. Chem. Soc., Perkin Trans. 2* **1986**, 75. (c) Fukuzumi, S.; Kuroda, S.; Goto, T.; Ishikawa, K.; Tanaka, T. *J. Chem. Soc., Perkin Trans. 2* **1989**, 1047. (d) Sawyer, D. T.; McCreery, R. L. *Inorg. Chem.* **1972**, *11*, 779. (e) Shinkai, S.; Nakao, H.; Honda, N.; Manabe, O. *J. Chem. Soc., Perkin Trans. 1* **1986**, 1825. (f) Tominami, T.; Ikeda, K.; Nabeshima, T.; Yano, Y. *Chem. Lett.* **1992**, 2293. (g) Shinkai, S.; Ishikawa, Y.; Manabe, O. *Bull. Chem. Soc. Jpn.* **1983**, *56*, 1694. (h) Shinkai, S.; Ishikawa, Y.; Shinkai, H.; Tsuno, T.; Makishima, H.; Ueda, K.; Manabe, O. *J. Am. Chem. Soc.* **1984**, *106*, 1801. (i) Fukuzumi, S.; Tani, K.; Tanaka, T. *J. Chem. Soc., Chem. Commun.* **1989**, 816.
- (12) (a) Fukuzumi, S.; Kuroda, S.; Tanaka, T. *J. Am. Chem. Soc.* **1985**, *107*, 3020. (b) Fukuzumi, S.; Kuroda, S.; Tanaka, T. *Chem. Lett.* **1984**, 1375.
- (13) Catalysis of photochemical reactions has been reviewed; see: (a) Wubbels, G. G. *Acc. Chem. Res.* **1983**, *16*, 285. (b) Fukuzumi, S.; Itoh, S. In *Advances in Photochemistry*; Neckers, D. C., Volman, D. H., von Bülow, G., Eds.; John Wiley & Sons: New York, 1999; Vol. 25, p 107. Although species which enhance the reactivity of photocatalysts do not appear to be well defined, such species may be called “co-catalysts” of photocatalysts.
- (14) Burgstaller, P.; Famulok, M. *J. Am. Chem. Soc.* **1997**, *119*, 1137.
- (15) (a) Shinkai, S.; Kameoka, K.; Ueda, K.; Manabe, O. *J. Am. Chem. Soc.* **1987**, *109*, 923. (b) Shinkai, S.; Nakano, H.; Ueda, K.; Manabe, O. *Tetrahedron Lett.* **1984**, *25*, 5295.
- (16) (a) Kagan, H. B.; Namy, J. L. *Tetrahedron* **1986**, *42*, 6573. (b) Molander, G. A. *Chem. Rev.* **1992**, *92*, 29. (c) Imamoto, T. *Lanthanides in Organic Synthesis*; Katritzky, A. R., Meth-Cohn, O., Rees, C. W., Eds.; Academic Press: London, 1994. (d) Kobayashi, S. *Synlett* **1994**, 689. (e) Marshmann, R. W. *Aldrichim. Acta* **1995**, *28*, 77. (f) Inanaga, J.; Yamaguchi, M. In *New Aspects of Organic Chemistry*; Yoshida, Z., Shiba, T., Ohshiro, Y., Eds.; VHC: New York, 1989; Chapter 4, p 55. (g) Molander, G. A.; Harris, C. R. *Chem. Rev.* **1996**, *96*, 307. (h) Shibasaki, M.; Sasai, H.; Arai, T. *Angew. Chem., Int. Ed. Engl.* **1997**, *36*, 1236.
- (17) (a) Kobayashi, S.; Nagayama, S.; Busujima, T. *Chem. Eur. J.* **2000**, *6*, 3491. (b) Kobayashi, S.; Nagayama, S.; Busujima, T. *J. Am. Chem. Soc.* **1998**, *120*, 8287. (c) Kobayashi, S.; Ishitani, H. *J. Am. Chem. Soc.* **1994**, *116*, 4083. (d) Markó, I. E.; Evans, G. R. *Tetrahedron Lett.* **1994**, *35*, 2771. (e) Kawada, A.; Mitamura, S.; Kobayashi, S. *Chem. Commun.* **1996**, 183. (f) Kobayashi, S.; Araki, M.; Hachiya, I. *J. Org. Chem.* **1994**, *59*, 3758. (g) Kobayashi, S.; Araki, M.; Hachiya, I. *J. Org. Chem.* **1994**, *59*, 3758. (h) Ishihara, K.; Kubota, M.; Kurihara, H.; Yamamoto, H. *J. Org. Chem.* **1996**, *61*, 4560. (i) Ishihara, K.; Kubota, M.; Kurihara, H.; Yamamoto, H. *J. Am. Chem. Soc.* **1995**, *117*, 4413, 6639. (c) Nagayama, S.; Kobayashi, S. *Angew. Chem., Int. Ed. Engl.* **2000**, *39*, 567. (d) Kobayashi, S.; Nagayama, S. *J. Am. Chem. Soc.* **1998**, *120*, 2985. (e) Kobayashi, S.; Hachiya, I.; Araki, M.; Ishitani, H. *Tetrahedron Lett.* **1993**, *34*, 3755. (f) Kawada, A.; Mitamura, S.; Kobayashi, S. *Synlett* **1994**, 545. (g) Kobayashi, S.; Moriwaki, M.; Hachiya, I. *J. Chem. Soc., Chem. Commun.* **1995**, 1527. (h) Kobayashi, S.; Nagayama, S. *J. Org. Chem.* **1996**, *61*, 2256. (i) Kobayashi, S.; Nagayama, S. *J. Am. Chem. Soc.* **1996**, *118*, 8977. (j) Bisi Castellani, C.; Carugo, O.; Giusti, M.; Leopizzi, C.; Perotti, A.; Invernizzi Gamba, A.; Vidari, G. *Tetrahedron* **1996**, *52*, 11045. (k) Lacôte, E.; Renaud, P. *Angew. Chem., Int. Ed. Engl.* **1998**, *37*, 2259.
- (19) Kyogoku, Y.; Yu, B. S. *Bull. Chem. Soc. Jpn.* **1969**, *42*, 1387.
- (20) (a) Hatchard, C. G.; Parker, C. A. *Proc. R. Soc. London, Ser. A* **1956**, *235*, 518. (b) Calvert, J. G.; Pitts, J. N. In *Photochemistry*; Wiley: New York, 1966; p 783.
- (21) (a) Forsberg, J. H.; Spaziano, V. T.; Balasubramanian, T. M.; Liu, G. K.; Kinsley, S. A.; Duckworth, C. A.; Poteruca, J. J.; Brown, P. S.; Miller, J. L. *J. Org. Chem.* **1987**, *52*, 1017. (b) Kobayashi, S.; Hachiya, I. *J. Org. Chem.* **1994**, *59*, 3590. (c) Kobayashi, S.; Hachiya, I.; Ishitani, H.; Araki, M. *Synlett* **1993**, 472. (d) Thom, K. F. U.S. Patent 3,615,169, 1971; *Chem. Abstr.* **1972**, *76*, 5436a.
- (22) Wallenfels, K.; Gellrich, M. *Chem. Ber.* **1959**, *92*, 1406.
- (23) Perrin, D. D.; Armarego, W. L. F. *Purification of Laboratory Chemicals*; Butterworth-Heinemann: Oxford, 1988.
- (24) Mair, R. D.; Graupner, A. *J. Anal. Chem.* **1964**, *36*, 194.
- (25) Patz, M.; Mayr, H.; Maruta, J.; Fukuzumi, S. *Angew. Chem., Int. Ed. Engl.* **1995**, *34*, 1225.
- (26) Mann, C. K.; Barnes, K. K. *Electrochemical Reactions in Non-aqueous Systems*; Marcel Dekker: New York, 1990.
- (27) Becke, A. D. *J. Chem. Phys.* **1993**, *98*, 5648.
- (28) Frisch, M. J.; Trucks, G. W.; Schlegel, H. B.; Scuseria, G. E.; Robb, M. A.; Cheeseman, J. R.; Zakrzewski, V. G.; Montgomery, J. A., Jr.; Stratmann, R. E.; Burant, J. C.; Dapprich, S.; Millam, J. M.; Daniels, A. D.; Kudin, K. N.; Strain, M. C.; Farkas, O.; Tomasi, J.; Barone, V.; Cossi, M.; Cammi, R.; Mennucci, B.; Pomelli, C.; Adamo, C.; Clifford, S.; Ochterski, J.; Petersson, G. A.; Ayala, P. Y.; Cui, Q.; Morokuma, K.; Malick, D. K.; Rabuck, A. D.; Raghavachari, K.; Foresman, J. B.; Cioslowski, J.; Ortiz, J. V.; Baboul, A. G.; Stefanov, B. B.; Liu, G.; Liashenko, A.; Piskorz, P.; Komaromi, I.; Gomperts, R.; Martin, R. L.; Fox, D. J.; Keith, T.; Al-Laham, M. A.; Peng, C. Y.; Nanayakkara, A.; Gonzalez, C.; Challacombe, M.; Gill, P. M. W.; Johnson, B.; Chen, W.; Wong, M. W.; Andres, J. L.; Gonzalez, C.; Head-Gordon, M.; Replogle, E. S.; Pople, J. A. *Gaussian 98 (Revision A.7)*; Gaussian, Inc.: Pittsburgh, PA, 1998.
- (29) Fukuzumi, S.; Kondo, Y.; Mochizuki, S.; Tanaka, T. *J. Chem. Soc., Perkin Trans. 2* **1989**, 1753.
- (30) The  $K_1$  and  $K_2$  values are determined within experimental error of  $\pm 10\%$  judging from the linearity of the plots.
- (31) (a) Wessiak, A.; Bruce, T. C. *J. Am. Chem. Soc.* **1983**, *105*, 4809. (b) Pokola, A.; Jorns, M. S.; Vargo, D. J. *J. Am. Chem. Soc.* **1982**, *104*, 5466.
- (32) (a) Heelis, P. F.; Parsons, B. J.; Phillips, G. O.; McKeller, J. F. *Photochem. Photobiol.* **1981**, *33*, 7. (b) Grodowski, M. S.; Veyret, B.; Weiss, K. *Photochem. Photobiol.* **1977**, *26*, 341.
- (33) Fukuzumi, S.; Okamoto, T.; Otera, J. *J. Am. Chem. Soc.* **1994**, *116*, 5503.
- (34) In the case of flavin, the lowest excited state may also have the  $\pi, \pi^*$  character.
- (35) Since metal ions employed in this study are diamagnetic, there is no possibility of paramagnetic quenching.
- (36) The agreement also indicates that there is no equilibrium in the excited state between  $^1\text{Fl}^*$  and the  $\text{Sc}^{3+}$  complexes because of the short lifetime of the excited state.
- (37) Traber, R.; Vogelmann, E.; Schreiner, S.; Werner, T.; Kramer, H. E. A. *Photochem. Photobiol.* **1981**, *33*, 41.
- (38) (a) Rehm, D.; Weller, A. *Isr. J. Chem.* **1970**, *8*, 259. (b) Rehm, D.; Weller, A. *Ber. Bunsen-Ges. Phys. Chem.* **1969**, *73*, 834.
- (39) Fukuzumi, S.; Fujita, M.; Otera, J.; Fujita, Y. *J. Am. Chem. Soc.* **1992**, *114*, 10271.
- (40) Large positive shift of the anodic peak potential ( $\Delta E_{\text{red}}^{\text{p}} = 400$  mV) of the ground-state riboflavin due to the complex formation with  $\text{La}^{3+}$  was observed in DMSO; see ref 11d.
- (41) Fukuzumi, S.; Itoh, S.; Komori, T.; Suenobu, T.; Ishida, A.; Fujitsuka, M.; Ito, O. *J. Am. Chem. Soc.* **2000**, *122*, 8435.
- (42) Patz, M.; Kuwahara, Y.; Suenobu, T.; Fukuzumi, S. *Chem. Lett.* **1997**, 567.
- (43) Fukuzumi, S.; Suenobu, T.; Patz, M.; Hirasaka, T.; Itoh, S.; Fujitsuka, M.; Ito, O. *J. Am. Chem. Soc.* **1998**, *120*, 8060.
- (44) The  $\text{BNA}^{\bullet}$  radical produced by the C–C bond cleavage in  $(\text{BNA})_2^{+}$  can reduce the electron acceptor, resulting in formation of two equivalents of the radical anion in the photoinduced electron transfer from  $(\text{BNA})_2$  to the electron acceptor.<sup>42,43</sup>
- (45) Niemz, A.; Imbriglio, J.; Rotello, V. M. *J. Am. Chem. Soc.* **1997**, *119*, 887.
- (46) There are the spin densities calculated using the density functional calculation at the B3LYP/6-311++G\*\* level on the nitrogen atoms ( $\text{N}^5$  and  $\text{N}^{10}$ ) and carbon atoms ( $\text{C}^6$ ,  $\text{C}^7$ ,  $\text{C}^8$ , and  $\text{C}^9$ ) where the hyperfine splitting due to the nitrogens and protons bound to the carbons is observed. It should be noted that there is almost no spin density on carbonyl oxygens with which  $\text{Sc}^{3+}$  binds.
- (47) The main difference between the ESR spectra of  $\text{Fl}^{\bullet-}$  and  $\text{Fl}^{\bullet-} - 2\text{Sc}^{3+}$  is a significant decrease in the  $a(\text{H}^{\text{p}})$  value in  $\text{Fl}^{\bullet-} - 2\text{Sc}^{3+}$  as compared to the value in  $\text{Fl}^{\bullet-}$ .
- (48) The transient absorption band due to  $p\text{-ClC}_6\text{H}_4\text{CHOH}^{\bullet}$  does not appear in the wavelength region in Figure 7a.
- (49) Fukuzumi, S.; Okamoto, T. *J. Chem. Soc., Chem. Commun.* **1994**, 521.
- (50) (a) Foote, C. S. *Acc. Chem. Res.* **1968**, *1*, 104. (b) Kearns, D. R. *Chem. Rev.* **1971**, *71*, 395. (c) Foote, C. S. In *Free Radicals in Biology*; Pryor, W. A., Ed.; Academic Press: New York, 1976; Vol. 2, p 85.